Purdue University
Purdue e-Pubs

International Refrigeration and Air Conditioning Conference

School of Mechanical Engineering

2016

Airside Performance Correlations and Optimal Heat Pump Heat Exchanger Designs Based on 0.5mm-2mm Finless Round Tube Bundles

Daniel Bacellar
University of Maryland, United States of America, dfbace@umd.edu

Vikrant Aute
University of Maryland, United States of America, vikrant@umd.edu

Reinhard Radermacher
University of Maryland, United States of America, raderm@umd.edu

Airside Performance Correlations and Optimal Air-Conditioning Heat Exchanger Designs Based on 0.5mm-2mm Finless Round Tube Bundles

Daniel BACELLAR[1], Vikrant AUTE[2]*, Reinhard RADERMACHER[3]

[1,2,3]Center for Environmental Energy Engineering
Department of Mechanical Engineering, University of Maryland
College Park, MD 20742 USA
[1]Tel: 301-405-7314, [2]Tel: 301-405-8726, [3]Tel: 301-405-5286
Email: [1]dfbace@umd.edu, [2]vikrant@umd.edu, [3]raderm@umd.edu

* Corresponding Author

ABSTRACT

The use of small diameter tubes in air-to-refrigerant heat exchangers has significant advantages, which include increase in heat transfer coefficient, reduction in size, reduction in material or weight and reduction in refrigerant charge. However, there are no airside correlations for small diameter tubes below 2.0mm in the literature. Furthermore, conventional empirical correlation development relies on testing of samples, which is inherently time consuming, expensive and has a limited range of applicability. This paper presents equations for airside friction and heat transfer characteristics for bare tube air-to-refrigerant Heat eXchangers (HX) with tube diameters ranging from 0.5mm to 2mm, and are valid for 2 to 40 rows of tubes in both staggered and inline arrangements. The correlations presented in this article are developed based on comprehensive CFD simulations for a large design space and include experimental validation. More than 80% of source data can be predicted within 10% error and more than 90% within 20% error. In this paper we use these correlations to optimize the condenser and evaporator of a 3 ton air-conditioning unit using R410A as the working fluid. The HX optimization framework uses a Multi-Objective Genetic Algorithm (MOGA) and an in-house HX design tool based on a segmented ε-NTU method. The ultimate goal of optimizing these HX's is to obtain better system performance. Therefore, the HX optimization targets the reduction of thermal resistance resulting in a smaller approach temperature and reduced pressure lift. A theoretical analysis showed that the maximum COP improvement is of 29%, however a 10% improvement is possible with realistic approach temperatures. The optimum HX's not only deliver the higher COP but are at least 50% more compact, 80% less material volume, have smaller face areas and reduced the overall system charge in 20%.

1. INTRODUCTION

There are a significant number of publications investigating experimentally, analytically and numerically the thermal-hydraulic performance of gas flow over tube banks. The interest is evident from its wide application from industrial processes to residential heating and cooling.

Grimison (1937), then later Žukauskas (1972) presented, perhaps, the most comprehensive experimental studies on the subject including the development of empirical correlations. Žukauskas (1972) correlations are the most commonly used even nowadays. Starting in the late 1970's numerical approaches became popular, especially as computational capabilities keep on continuously increasing. Launder and Massey (1978) proposed a cost-effective computational method for laminar flow prediction over staggered tubes and compared against experimental data from Bergelin et al. (1952). Fujii et al. (1984) focused on the in-line configuration for fixed number of tube rows and constant tube pitch ratios, varying only the Reynolds number. Wung and Chen (1989a,b) presented a parametric analysis on Prandtl and Reynolds numbers and correlated their numerical data into expressions. Their analysis however did not account for geometry variables. Dhaubhadel et al. (1987) solved the same problem as Fujii et al. (1984) but for staggered arrangement. Beale and Spalding (1999) investigated unsteady flow on both in-line and staggered tube banks. Wilson and Bassiouny (2000) studied single and double row tube banks parameterizing tube pitches and Reynolds number. They also compared their results with empirical data. Buyruk (2002) made a similar study using fine grid resolutions.

On an analytical approach Khan et al. (Khan, Culham, & Yovanovich, 2006) developed alternate equations for heat transfer and friction for both inline and staggered arrangements. Their equations are limited to tube pitch ratios ranging from 1.05 to 3. They found good agreement with Grimison (1937) and Žukauskas (1972) for a 16.4mm tube diameter. There are no explicit evidences that the available equations in the literature can predict the thermal-hydraulic performances for tube banks using small tube diameters (below 7.0mm). A recent study from Bacellar et al. (2016) presented new equations for airside thermal-hydraulic characteristics prediction for bare tube bundle with diameters ranging from 0.5mm to 2.0mm, in staggered arrangement.

The main advantages of reducing the tube diameter include high surface area to volume ratio, significant material reduction, refrigerant side volume reduction, which would result in refrigerant charge reduction; but more importantly a significant enhancement in heat transfer coefficient (Paitoonsurikarn et al., 2000; Kasagi et al., 2003; Bacellar et al., 2015). In other words, with smaller tubes the need for fins becomes less significant or even dispensable. Some manufacturers are already producing tubes with 4.0mm, 5.0mm and 7.0mm, however the use of fins is still required. For such diameters the majority of the literature focus on the refrigerant side (e.g. (Huang, et al., 2010)), with few studies including the airside (e.g. (Wu et al., 2012)).

Microchannel HX's have proven to be an excellent HX for vapor compression applications. In this paper, we present the optimization of indoor and outdoor units for an R410A 3-ton system operating in cooling mode. The optimized HX's are bare tube bundles with diameters ranging from 0.5mm to 2.0mm in both staggered and in-line arrangements. For the latter we briefly present the correlation development using the same procedure in (Bacellar et al., 2016). The baseline HX's are louvered fin-and-tube HX's using tube diameters of 7.0mm and 9.5mm for the outdoor and indoor units respectively. The baseline system was modeled and verified against the rating point.

2. METHODOLOGY

This paper presents the application of a design framework for evaporators and condensers for a 3-ton system. The framework (Figure 1) is split into four parts, and each is described in detail in the following sections along with the according results. The first part is the problem specification, where we define the design characteristics such as operating conditions, capacity and flow arrangements. The following is the actual design and optimization; in this part, we present the performance evaluation objectives and the tools used to perform the optimization. This work focuses on tube diameters below 2.0mm, which the existing correlations cannot accurately predict. To overcome this limitation we have developed CFD-based correlations for a large design space allowing great computational time savings during the optimization. The third part presents a brief formulation for a Multi-Attribute Utility Function (MAUF) used to select the best alternative from the Pareto sets. The last part is the evaluation of the optimum HX's in the system context and their comparison to the baseline.

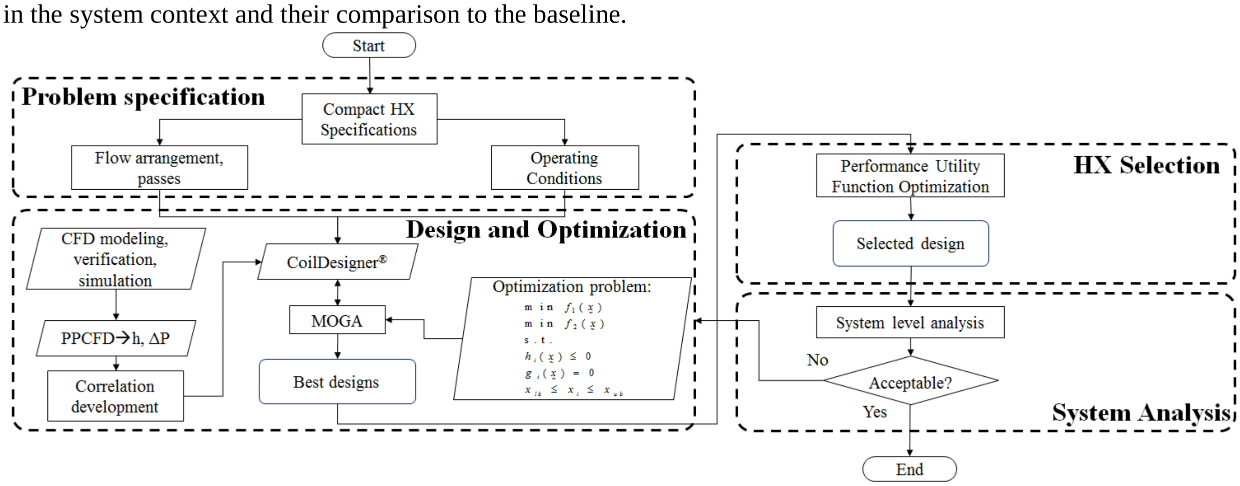

Figure 1: Design framework.

3. PROBLEM SPECIFICATION

The baseline for this study is a R410A 3-ton system, operating in cooling mode. The baseline cycle was modeled, simulated using an in-house code (Winkler et al., 2008) and verified against the rating design point for the cooling mode. The overall system rating and numerical simulation are presented in Table 1.

Ultimately, the purpose of optimizing the HX is to improve the system's performance. There are two possible ways to tackle this problem; one is by optimizing the COP of the cycle, the other is to design the HX's for a new set of operating conditions that would result in higher COP. In this paper, we choose the second approach. To evaluate a hypothetical improved cycle (Figure 2) we apply factors to the saturation pressures, and refrigerant pressure drops. The assumptions include same air heat capacitance rates and inlet temperatures, same superheating, same sub-cooling, and same isentropic and volumetric efficiencies. The constraint variables are the outlet approach temperatures and these are limited to 1°C or higher. The analyses showed that by reducing the high saturation pressure in 6%, increasing the low saturation pressure in 1.05% and reducing the refrigerant pressure drop in 20% the COP can be improved by 10% (Table 1). Assuming no pressure drop and 0°C approach temperatures on both HX's, the maximum hypothetical COP improvement would be of 28.8% by reducing the high pressure by 12% and increasing the lower pressure by 4%.

Table 1: 3-ton system, cooling mode.

Cycle	Charge	COP*	COP	Q	Sub-cooling	Super heating	Ref. ṁ	Evap. AFR	Cond. AFR
	kg	-	-	kW	K	K	kg/s	m^3/s	m^3/s
Baseline (rated)	5.557	4.507	3.900	10.029	5.447	3.890	0.06224	0.505	1.84
Baseline (simulated)	4.907	4.506	3.858	10.025	5.445	3.901	0.06168	0.505	1.84
Improved system	-	4.992	4.210**	10.030	5.447	3.911	0.05994	0.505	1.84

**w/o fan power **using rated fan power*

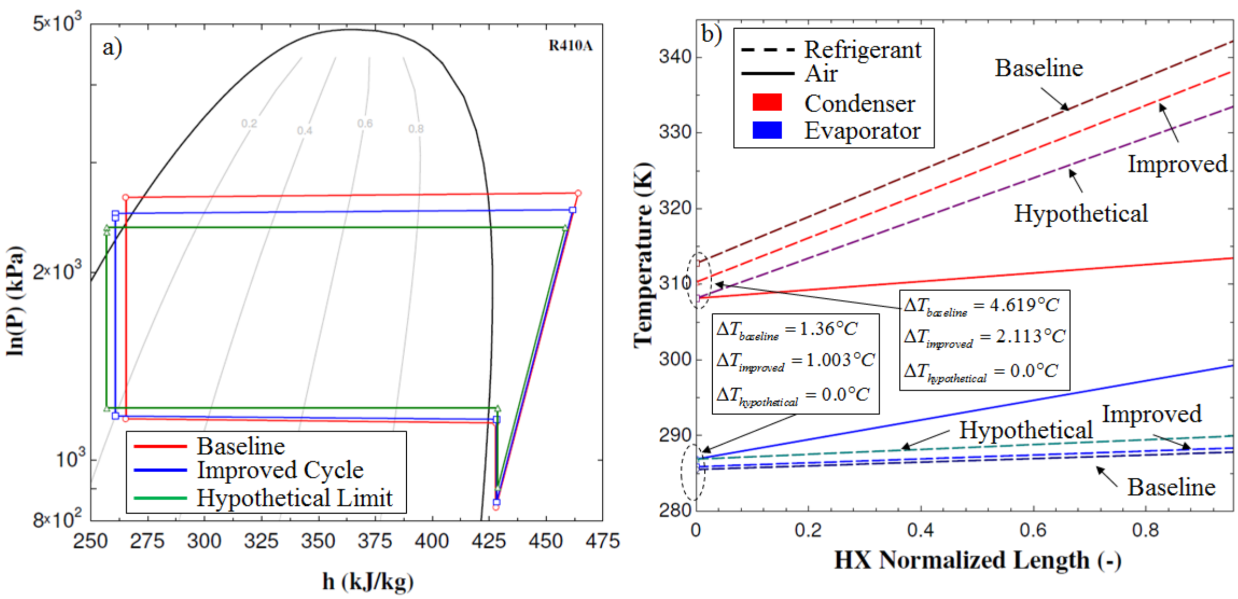

Figure 2: 3-ton system analysis: a) P-h diagram; b) Temperature profiles.

Table 2: HX performances for both baseline and improved cycles.

HX	Evaporator						Condenser					
Metric	Q W	P_{sat} kPa	ΔP_{ref} kPa	UA W/K	ΔT_{ml} K	ΔP_{air} Pa	Q W	P_{sat} kPa	ΔP_{ref} kPa	UA W/K	ΔT_{ml} K	ΔP_{air} Pa
Baseline	10.025	1166	18	2061.52	4.86	57.2*	12.251	2682	41	912.30	13.43	4.0**
Improved	10.030	1178	13	2351.66	4.26	N/A	12.040	2521	33	1269.19	9.49	N/A

**Rated value **Calculated value* (Wang et al., 2001)

The design problem for this study is, therefore, optimizing HX's that have the performance characteristics to deliver the 3-ton capacity under the improved operating conditions. The HX's consist of a tube bundle, for both staggered and in-line arrangements, in crossflow configuration. The tube circuiting is similar to Microchannel HX's, i.e. connected to headers, with up to 3 passes (Figure 3).

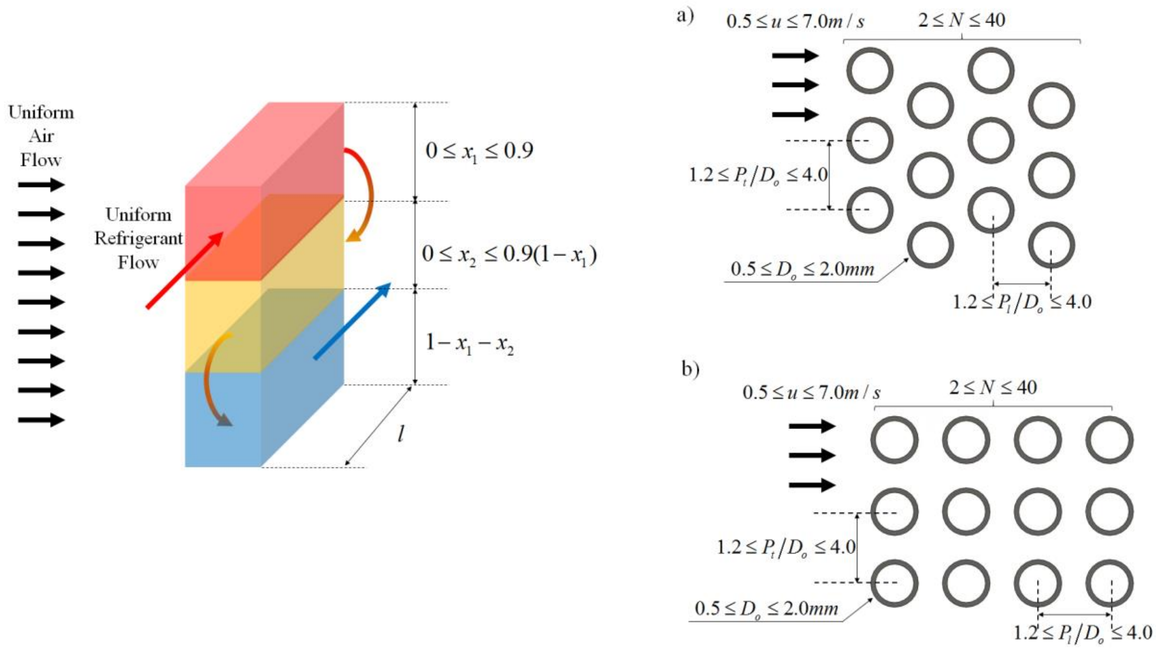

Figure 3: HX's design space: a) staggered; b) in-line.

4. DESIGN AND OPTIMIZATION

4.1 Correlation development

The airside performance is evaluated using the novel correlations proposed for tube bundles within the design space specified (Figure 3). For the staggered arrangement the equations were published by Bacellar et al. (Bacellar et al., 2016). In this, paper we present the correlations for the in-line arrangement.

The source data for the fitted equations are purely numerical using CFD. The Design of Experiment consists of 900 samples generated using Latin Hypercube Sampling (LHS) (McKay, Beckman, & Conover, 1979). The simulations are carried out in an automated fashion (Parallel Parameterized CFD (PPCFD) (Abdelaziz et al., 2010)). The correlations proposed are modifications of existing correlations applied to larger range of tube diameters. The coefficients are determined by solving the minimum of the square differences sum (equation 1).

$$e_{ss} = \sum_i \left(\phi_{i,correlation} - \phi_{i,CFD}\right)^2, \phi = j, f \tag{1}$$

4.1.1 CFD Models

The CFD computational domain is a two dimensional cross section segment of the HX, assuming any end effects to be negligible. The inlet boundary has uniform velocity and uniform temperature (300K), whereas the outlet boundary is at constant atmospheric pressure. The upper and lower boundaries are periodic, and the tube walls are at constant temperature of 340K. The fluid properties use ideal gas model, and the turbulence is evaluated using the k-ε relizable model. The convergence criteria used is 10^{-5}. The near wall region mesh is a fine map scheme with growing layers at a ratio of 1.2 (Figure 4). The core of the computational domain is a pave mesh scheme with an average element size equal to the last row of the boundary layer mesh.

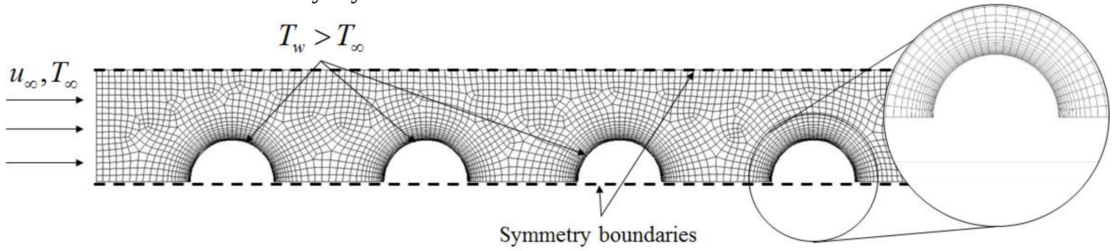

Figure 4: CFD computational domain and mesh.

4.2.2 CFD Data Reduction

Since the CFD models serve to determine the airside thermal and hydraulic resistances, there is no need to account for additional thermal resistances. Thus with constant wall temperature, the capacitance ratio yields C_{min} / C_{max} = 0, then the heat transfer coefficient can be easily calculated through ε-NTU method as per equations (1-3). The pressure drop is determined as the difference between inlet and outlet static pressures, assuming that local losses are negligible.

$$NTU = -\ln(1-\varepsilon) = -\ln\left[1-(T_{out}-T_{in})/(T_{wall}-T_{in})\right] \tag{2}$$

$$h = UA/A_o = NTU \cdot C_{\min}/A_o \tag{3}$$

$$j = h\,\mathrm{Pr}^{2/3}/(\rho u_c c_p) \tag{4}$$

$$f = A_c\rho_m/(A_o\rho_{in})\left[2\Delta P\rho_{in}/(\rho_m u_c)^2 + (1-\sigma^2)(\rho_{in}/\rho_{out}-1)\right] \tag{5}$$

4.2.3 Proposed Equations

Four subsets of correlations for each performance factor is proposed according to the number of tube rows. The correlations coefficients are presented in Table 3, and the verification against the source data is presented in Figure 5.

$$j = c_1\,\mathrm{Re}_{D_o,c}^{p_1} N^{p_2} (P_l/D_o)^{p_3} (P_t/D_o)^{p_4} (P_l/P_t)^{c_2} \tag{6}$$

$$f = c_1\,\mathrm{Re}_{D_o,c}^{p_1} (P_t/P_l)^{p_2} (P_l/D_o)^{p_3} (P_t/D_o)^{p_4} N^{c_2} \tag{7}$$

$$\mathrm{Re}_{D_o,c} = \rho u_c D_o/\mu \tag{8}$$

$$p_1 = c_3 + c_4 N/\ln(\mathrm{Re}_{D_o,c}) + c_5 \ln\left[N (P_l/D_o)^{c_6}\right] \tag{9}$$

$$p_2 = c_7 + c_8/\ln(\mathrm{Re}_{D_o,c})(P_l/D_o)^{c_9} \tag{10}$$

$$p_3 = c_{10} + c_{11} N/\ln(\mathrm{Re}_{D_o,c}) \tag{11}$$

.

$$p_4 = c_{12} + c_{13}\ln\left(\mathrm{Re}_{D_{o,c}}/N\right) \tag{12}$$

Table 3. Correlations Coefficients.

	j				f			
N	2-9	10-24	25-34	35-40	2-9	10-24	25-34	35-40
c_1	6.808	1.079	4.072	0.059	4.358	0.834	3.627	1.905
c_2	-0.019	0.283	0.819	0.732	-1.500	0.160	-1.255	-3.427
c_3	-0.865	-0.694	-1.668	0.300	-0.593	-0.614	-0.947	1.841
c_4	-0.072	0.018	-0.151	0.025	-0.058	-0.045	0.149	0.309
c_5	0.215	0.091	0.476	-0.099	0.210	0.068	0.080	-0.617
c_6	-0.557	-0.671	-0.831	-0.012	-1.512	2.005	-4.952	0.395
c_7	-1.390	-0.925	-0.362	-0.514	-1.096	-0.720	4.492	0.313
c_8	2.861	2.297	1.130	0.665	4.546	0.138	10.000	10.000
c_9	-3.997	0.439	-0.234	1.116	-0.233	2.779	-2.034	-2.737
c_{10}	-0.114	0.359	-0.584	-0.081	-0.643	0.733	8.397	5.098
c_{11}	0.696	-0.056	0.446	0.003	0.941	0.147	-0.591	-0.649
c_{12}	-1.072	-1.739	-0.315	-0.806	0.144	-1.684	-3.116	1.814
c_{13}	0.285	0.393	0.541	-0.043	0.557	0.278	0.322	-0.228

4.2 Performance Evaluation Criteria

In this paper, we use the performance-degradation number (equation 13) as the Performance Evaluation Criteria (PEC). Typically, the performance of the HX is heavily focused on reducing the friction losses to the same thermal resistance. The performance-degradation number is one way to ensure the optimizer will seek the reduction of both thermal and hydraulic resistances.

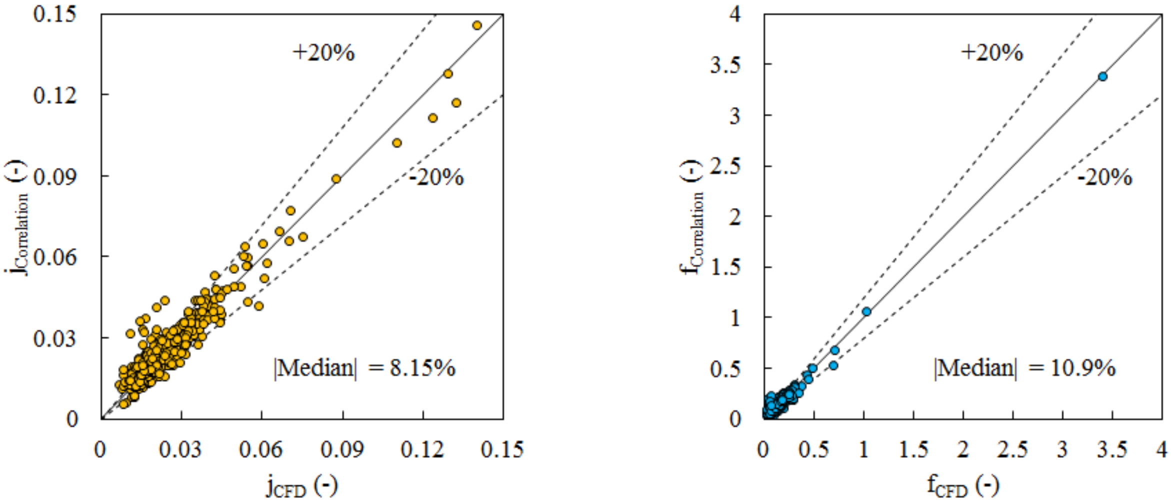

Figure 5: Correlation verification against source data.

$$\psi = NTU / N_s \tag{13}$$

In many applications, the envelope volume is not much of an issue as long as the design can satisfy potential limitations on tube length, face area and/or aspect ratio. The face area can be more critical since it can affect the cross section of an air duct, size of an equipment casing, or the size of the front of a car for example. Ultimately the metrics that evaluate better the geometrical aspects of a HX are the surface hydraulic diameter (equation 14), since it is inversely proportional to compactness, and the actual face area.

$$D_h = 4A_c / A_o\, d \rightarrow V / A_o = 4\sigma / D_h \tag{14}$$

4.3 Multi-objective optimization

Studies on HX optimization have now become very common, particularly since computational power is increasing at great strides along with improved CFD codes and optimization methods like Multi-Objective Genetic Algorithms (MOGA) (method used in this paper). An in-house code (Jiang et al., 2006) that allows modeling and simulation of various types of air-to-refrigerant HX's using a segmented ε-NTU approach is used for the present analysis. This tool, assisted by the new airside correlations, allows the optimizer to build and evaluate full sized HX designs. The optimization problem is described on Table 4.

Table 4: Optimization problem.

Optimization	Evaporator	Condenser
Objectives	min A_f max ψ (both)	
Constraints	$10.02 \leq Q \leq 10.04$kW $V_{HX} \leq 14{,}612$ cm³ $\Delta P_{air} \leq 50$ Pa $8.62 \leq \Delta P_{ref} \leq 13.78$ kPa $0.5 \leq u_{air} \leq 2.0$ m/s	$12.00 \leq Q \leq 12.05$kW $V_{HX} \leq 41{,}884$cm³ $\Delta P_{air} \leq 15$ Pa $20.84 \leq \Delta P_{ref} \leq 33.3$ kPa $0.5 \leq u_{air} \leq 1.2$ m/s
	0.61<AR<1.61 (both)	
Population Size	200	
Replacement (%)	10	
Max Iterations	750	

The optimization results are presented in Figure 6 in the next section, which includes the selection criteria.

5. HX SELECTION

To select the HX we developed a Multi-Attribute Performance Utility Function based on Scott and Antonsson (2005) method (equation 15). The single attribute utility functions are calculated using the exponential form (equation 16). One way to define shape factor (γ) is by assuming that for the median criteria values the utility is 0.5.

$$U(\underset{\sim}{x}) = \left(\frac{\sum w_i u(x_i)^p}{\sum w_i}\right)^{1/p}, \quad \text{if } p=0 \rightarrow U(\underset{\sim}{x}) = \left(\sum u(x_i)^{w_i}\right)^{1/\sum w_i} \tag{15}$$

$$u(x_i) = \frac{1-e^{-\gamma(x_i-a)}}{1-e^{-\gamma(b-a)}}, \quad \underset{\sim}{x} = \left[\psi, 4\sigma/D_h, A_f^{-1}\right], \quad a \le x_i \le b, \quad 0 \le u(x_i) \le 1 \tag{16}$$

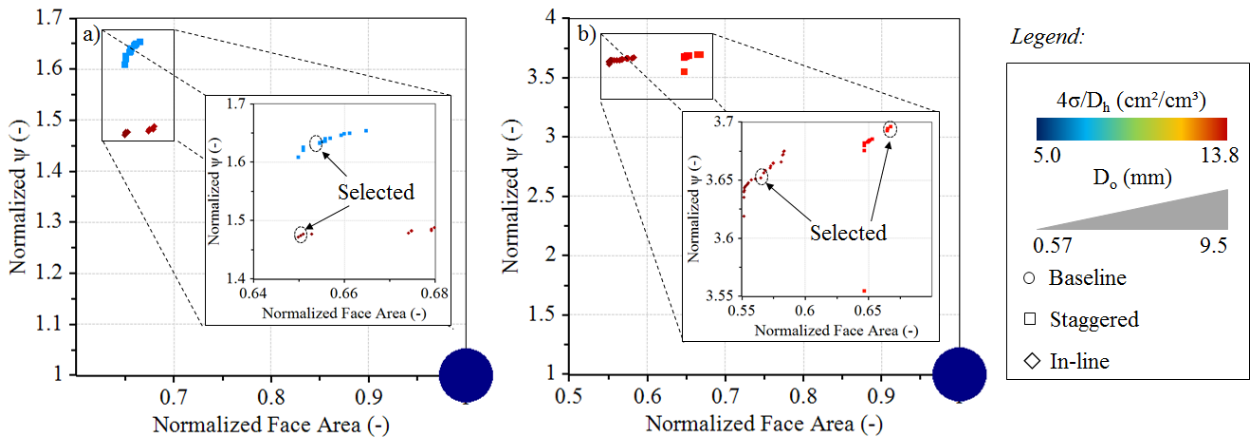

Figure 6: Optimization Results.

Table 5: Comparison of HX designs.

HX	Type	D_o mm	Banks -	d m	h m	l m	A_f m²	$4\sigma/D_h$ cm²/cm³	Matl' Vol. cm³
Baseline 1	Evaporator	9.5	4	0.076	1.12	0.43	0.48	6.79	3600
Baseline 2	Condenser	7.0	1	0.019	1.01	2.71	2.74	5.02	5900
Staggered 1	Evaporator	0.86	22	0.029	0.67	0.47	0.31	7.40	587
Staggered 2	Condenser	0.57	10	0.012	1.69	1.09	1.83	12.68	1194
In-line 1	Evaporator	0.70	18	0.026	0.71	0.44	0.31	13.75	615
In-line 2	Condenser	0.60	18	0.026	1.37	1.17	1.60	13.43	2266

Table 6: HX performance comparison.

HX	Evaporator						Condenser					
Metric	Q W	P_{sat} kPa	ΔP_{ref} kPa	UA W/K	ΔT_{ml} K	ΔP_{air} Pa	Q W	P_{sat} kPa	ΔP_{ref} kPa	UA W/K	ΔT_{ml} K	ΔP_{air} Pa
Baseline	10.025	1166	18	2061.5	4.86	57.2*	12.251	2682	41	912.3	13.43	4.0**
Expected	10.03	1178	13	2351.7	4.26	N/A	12.04	2521	33	1269.19	9.49	N/A
Staggered	10.038	1178	9.4	3061.1	3.28	44.9	12.05	2521	31.0	1307.3	9.22	9.97
In-line	10.038	1178	13.1	2839.6	3.53	33.7	12.049	2521	20.9	1304.8	9.23	11.00

**Rated value **Calculated value* (Wang, Lee, & Sheu, 2001)

6. SYSTEM ANALYSIS

In this section, we present the system level analysis. Four cycles are simulated with a combination of the optimum HX selected in the previous section. The purpose here is to investigate whether the desired cycle performance improvement can be achieved, in addition to the evaluation of the potential charge reduction when using small diameter tube HX's. All system simulations use the in-house code (Winkler et al., 2008) for vapor compression cycle analyses. It must be noted that the fan power was not taken into consideration since there is lack of information regarding the rated airside pressure drop in the condenser. If the predicted value of 4.0Pa is correct, then the fan power consumed in the new condensers can be twice or more as high as the baseline. If that were the case, then the total power consumed would be similar to the baseline and the real COP improvement would not reach 10%. The results are summarized in Figure 7and Table 7.

Table 7: Cycle analysis with optimized HX designs.

Cycle	Evaporator -	Condenser -	P_{sat} High kPa	P_{sat} Low kPa	Q kW	W_c kW	COP* -	Charge kg
Baseline	Baseline	Baseline	2682.00	1166.00	10.03	2.22	4.51	4.91
Expected	N/A	N/A	2521.00	1178.00	10.03	2.01	4.99	-
Cycle1	Staggered	Staggered	2534.05	1169.76	10.42	2.10	4.96	3.72
Cycle2	In-line	Staggered	2533.30	1170.81	10.40	2.10	4.95	3.73
Cycle3	Staggered	In-line	2530.61	1170.50	10.38	2.10	4.95	4.09
Cycle4	In-line	In-line	2531.43	1171.20	10.38	2.10	4.95	4.10

**w/o fan power*

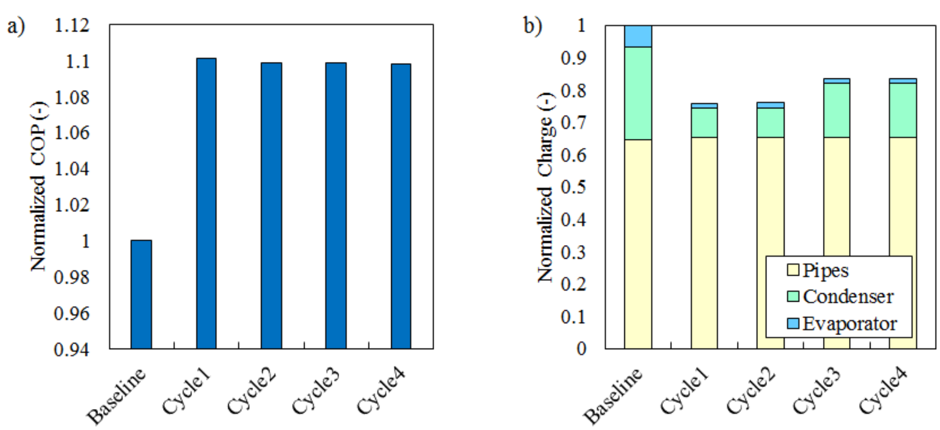

Figure 7: Cycle analysis – qualitative results: a) COP; b) Charge distribution.

7. CONCLUSIONS

This paper presented a comprehensive design framework and its application to evaporators and condensers using R410A for a 3-ton system. A parametric analysis showed a theoretical maximum COP improvement of 29%, however a more realistic scenario where the approach temperatures are at least 1°C would result in 10% better COP. The baseline HX's were already sized to have very low thermal resistance at a cost of size and material consumption. On the other hand, the potential improvement in terms of performance is limited. On section 4.1 we presented the new equations for thermal-hydraulic prediction for in-line bare tubes with diameters ranging from 0.5mm-2.0mm. These equations in addition to the ones for staggered equations presented in another publication were used to optimize the HX's. The performance-degradation number is a more robust way of balancing thermal and hydraulic resistances, when typically the second is favored over the first. The optimization problem formulation had the air pressure drop in the condenser constrained to a typical value of 15Pa. The baseline condenser has a predicted pressure drop of 4.0Pa. Since the rated value is unknown, the analysis disregarded the fan power, however, this can affect the real COP. The optimum HX's resulted in designs with tubes no larger than 0.86mm and several tube banks. The face area was reduced by at least 33% and the compactness was increased by a factor of approximately 2. The material volume reduction reached more than 80%. From a performance perspective, the thermal resistance was reduced by more than 30%, while the refrigerant pressure drop was reduced by at least 20%. The system analysis showed that the optimum designs matched quite well with the expected improvement. The new designs demonstrated a potential improvement in 10% in the COP (provided the fan power not to have a significant impact), while the charge was reduced in more than 20% for the whole system but more than 50% within the HX's.

NOMENCLATURE

A_c	Minimum free flow area	m²	Pl	Tube longitudinal pitch	mm
A_{fr}	Frontal face area	m²	Pr	Prandtl number	-
AFR	Airflow rate	m³/s	Pt	Tube transversal pitch	mm
A_o	Surface area	m²	Q	Heat transfer rate	W
AR	Aspect ratio	-	Re	Reynolds Number	-
C	Heat capacitance rate	W/K	T	Temperature	K
COP	Coefficient of Performance	-	u	Velocity	m/s
c_p	Specific heat	J/kg.K	U	Multi-Attribut Utility Function	-
d	Depth	m	u(x)	Single Attribute Utility Function	-
D_h	Surface hydraulic diameter	m	UA	Thermal conductance	W/K
D_o	Tube outer diameter	mm	uc	Maximum velociy	m/s
e	Error function	-	V	Volume	m³
f	Friction factor	-	V	Volume flow rate	m³/s
h	Heat transfer coefficient	W/m².K	$\dot{W}$	Compressor power	W
h	Height	m	ΔP	Pressure drop	Pa
j	Colburn factor	-	ΔTmax	Inlet appraoch temperature	K
l	Tube length	mm	ΔTml	Logarithmic Mean Temperature Difference	K
$\dot{m}$	Mass flow rate	kg/s	*Greek Letters*		
N	Nuber of tube banks	-	ρ	Density	kg/m³
Ns	Entropy generation units	-	ε	Effectiveness	-
NTU	Number of transfer units	-	μ	Dynamic viscosity	Pa.s
p	Norm order	-	σ	Contraction ratio (u/u_{max})	-
P	Pressure	Pa	ψ	Performance-degradation number	-

ACKNOWLEDGMENT

This work was supported by the United States Department of Energy Grant Number DE-EE0006114 and the Modeling and Optimization Consortium at the University of Maryland.

REFERENCES

Abdelaziz, O., Azarm, S., Aute, V., & Radermacher, R. (2010). Approximation-Assisted Optimization for Novel Compact Heat Exchanger Designs. *HVAC&R Research, 16*(5), 707-728.

Bacellar, D., Abdelaziz, O., Aute, V., & Radermacher, R. (2015). Novel heat exchanger design using Computational Fluid Dynamics and Approximation Assisted Optimization. *ASHRAE Winter Conference* (pp. 1-8). Chicago: ASHRAE.

Bacellar, D., Aute, V., Huang, Z., & Radermacher, R. (2016). Airside Friction and Heat Transfer Characteristics for Staggered Tube Bundle in Crossflow Configuration, with Diameters from 0.5mm to 2.0mm. *International Journal of Heat and Mass Transfer (in press)*.

Beale, S., & Spalding, D. (1999). A numerical study of unsteady fluid flow in in-line and staggered tube banks. *Journal of Fluids and Structures, 13*, 723-754.

Bergelin, O., Brown, G., & Doberstein, S. (1952). Heat transfer and fluid friction across banks of tubes - IV. *Transactions ASME, 74*, 953-960.

Buyruk, E. (2002). Numerical study of heat transfer characteristics on tandem cylinder, inline and staggered tube banks in crossflow of air. *International Communications of Heat and Mass Transfer, 29*, 355-366.

Dhaubhadel, M., Reddy, J., & Telionis, D. (1987). Finite element analysis of fluid flow and heat transfer for staggered banks of cylinders in crossflow. *International Journal of Numerical Methods Fluids, 7*, 1325-1342.

Fujii, M., Fujii, T., & Nagata, T. (1984). A numerical analysis of laminar flow and heat transfer of air in an in-line tube bank. *Numerical Heat Transfer, 7*, 89-102.

Grimison, E. (1937). Correlation and utilization of new data on flow resistances and heat transfer for cross flow of gases over tube banks. *Transactions ASME, 59*, 583-594.

Huang, X., Ding, G., Hu, H., Zhu, Y., Peng, H., Gao, Y., & Deng, B. (2010). Influence of oil on flow condensation heat transfer of R410A inside 4.18mm and 1.6mm inner diameter horizontal smooth tubes. *International Journal of Refrigeration*, 158-169.

Jiang, H., Aute, V., & Radermacher, R. (2006). CoilDesigner: A general purpose simulation and design tool for air-to-refrigerant heat exchangers. *International Journal of Heat and Mass Transfer, 29*, 601-610.

Kasagi, N., Suzuki, Y., Shikazono, N., & Oku, T. (2003). Optimal design and assessment of high performance micro bare-tube heat exchangers. *Proc. 4th Int. Conf. on Compact Heat Exchangers and Enhancement Technologies for the Process Industries.* Crete, Greece.

Khan, W., Culham, J., & Yovanovich, M. (2006). Convection heat transfer from tube banks in crossflow: Analytical approach. *International Journal of Heat and Mass Transfer, 49*, 4831–4838.

Launder, B., & Massey, T. (1978). The numerical prediction of viscous flow and heat transfer in tube banks. *Journal of Heat Transfer, 100*, 565-571.

McKay, M., Beckman, R., & Conover, W. (1979). A comparison of three methods for selecting values of input variables in the analysis of output from a computer code. *Technometrics*, *21*, 239-245.

Paitoonsurikarn, S., Kasagi, N., & Suzuki, Y. (2000). Optimal design of micro bare-tube heat exchanger. In P. Cheng (Ed.), *Proceedings of Symposium on Energy Engineering in the 21st Century*, *3*, pp. 972-979. Hong Kong.

Scott, M., & Antonsson, E. (2005). Compensation Weights for Tradeoffs in Engineering Design: Beyond Weighted Sum. *Journal of Mechanical Design*, 1045-1055.

Wang, C., Lee, W., & Sheu, W. (2001). A comparative study of compact enhanced fin-and-tube heat exchangers. *International Journal of Heat and Mass Transfer*, 3565-3573.

Wilson, A., & Bassiouny, M. (2000). Modeling of heat transfer for flow across tube banks. *Chemical Engineering and Processing, 39*, 1-14.

Winkler, J., Aute, V., & Radermacher, R. (2008). Comprehensive Investigation of Numerical Methods in Simulating a Steady-State Vapor Compression System. *International Journal of Refrigeration*, 930-942.

Winkler, J., Aute, V., & Radermacher, R. (2008). Comprehensive investigation of numerical methods in simulating steady-state vapor compression systems. *International Journal of Refrigeration, 31*, 930-942.

Wu, W., Ding, G., Zheng, Y., Gao, Y., & Song, J. (2012). Principles of designing fin-and-tube heat echanger withsmaller tube for air conditioning. *International Refrigeration and Air Conditioning Conference.* Lafayette, IN.

Wung, T., & Chen, C. (1989). Finite Analytic Solution of Convective Heat Transfer for Tube Arrays in Crcssflow: Part I-Flow Field Analysis. *Journal of Heat Transfer, 111*, 633-640.

Wung, T., & Chen, C. (1989). Finite analytic solution of convective heat transfer for tube arrays in crossflow: Part II - Heat transfer analysis. *Journal of Heat Transfer*, 641-648.

Žukauskas, A. (1972). Heat Transfer from Tubes in Cross Flow. In *Advances in Heat Transfer.* New York: Academic Press.